Chromatographia (2020) 83:1145–1151
https://doi.org/10.1007/s10337-020-03932-w

ORIGINAL

High Sensitive Visual Protein Detection by Microfluidic Lateral Flow Assay with On-Stripe Multiple Concentration

Shiyong Yu[1] · Weiwei Sun[1] · Pengjie Zhang[1] · Yu Chen[1] · Liben Yan[1] · Lina Geng[1] · Deng Yulin[1]

Received: 5 May 2020 / Revised: 21 June 2020 / Accepted: 3 July 2020 / Published online: 13 July 2020

Abstract

Lateral flow assays (LAFs) especially integrated with a microfluidic chip, provides a simple, rapid, user-friendly, potable robust, and cost-effective technology for broad assays. However, this technology suffers from low sensitivity. In this paper, one kind of automatic roller of tap, which can be precisely controlled to replace sample tap was integrated into the microfluidic LAFs platform. And then, on-stripe repeated injection and concentration were realized with this simple mechanic unit. The minimum detection concentration for human chorionic gonadotropin (HCG) was 1.26 ng/mL, comparable with literature using complex enzyme/chemical reaction-based signal amplification. The linear relationship between the signal intensity and enrichment times reflected the good reproducibility of the novel device. At the same time, the good linear relationship between the predicted accumulation quantity of HCG and the gray value of bands is very meaningful for quantitative detection. Consequently, this novel universal approach shows great potential in the rapid trace analysis and broaden the application of LAFs with its attractive characteristics.

Keywords Lateral flow · Microfluidic chip · Sensitivity · HCG

Introduction

Being rapid, inexpensive, easy-to-manufacture and user-friendly, lateral flow assays (LFAs) have usually been the first technology to be considered in a range of fields, including medical diagnostics, bedside analysis, food safety, and environmental safety for biochemical analytes, such as proteins, glycolipids, lipids, and nucleic acids [1–5]. Microfluidics technology brings great potential by providing integration, high-throughput, fast analysis time, portability, and small reagent volume. Taking advantage of the microfluidics, there have been a lot of efforts to integrated lateral flow assays (LAFs) with the microfluidic device to realize integrated assay platform with multifunction, for example, an integrated rotary microfluidic system with DNA extraction, loop-mediated isothermal amplification, and lateral flow strip based detection for point-of-care pathogen diagnostics [6]. At the same time, various microfluidic elements such as hydraulic resistors [7, 8] valves [9], and advanced features for liquid flow control [10] were also introduced into LAFs. However, due to the limit in the space of LFAs and microfluidic chip, the outstanding issues on detection sensitivity remain unsettled, which is an urgent problem in their practical application. Especially in the case of real sample analysis, such as human body fluids, the detection of low-abundance proteins in serum still face a great challenge. Non-integrated sample preparation steps were normally needed, which comprised the efficiency and equipment free advantage owned by LFAs. There were extensive researches in the enhancement of sensitivity without the special sample preconcentration beforehand [11–13], such as the improvement of capture reagent immobilization [14], the transport performance [15–23], the novel labels [24–27], signal amplification [28, 29] and readers [1, 13, 30–32]. Different from the focuses on the existing LFAs components using complex enzyme/chemical reaction-based signal amplification as literature, in this paper high sensitive microfluidic lateral flow visual assay of protein was realized with the aid of automatic roller to achieve automatic on-stripe repetitive injection and then multiple concentration.

✉ Shiyong Yu
shiyong0320@163.com

[1] School of Life Science and Technology, Beijing Institute of Technology, 5 South3 Zhongguancun Street, Haidian, Beijing, China

Materials and Methods

Materials and Reagents

Human chorionic gonadotropin (HCG) was ordered from Shanghai Linc-Bio Science Co. LTD. Water was purified and deionized with a Milli-Q system (Millipore, America). The micro peristaltic pump was ordered from LongerPump. AB adhesive was ordered from Ausbond, USA. The double-side adhesive was ordered from 3 M China co. LTD. PVC board purchased from Shanghai Jiening Biological co. LTD. Risym micro gear motor purchased from Shenzhen Kebiwei Electronics co. LTD. Photos were taken by a cellphone ordered from Xiaomi Corporation.

The Structure of the Microfluidic Device

Figure 1a is the 3D design drawing of the entire device. As shown in Fig. 1b, the interior structure consists of two parts: microfluidic section and control section. There are two rollers on the chip, just like the ones in a tape, roller A is the driving one, and roller B is the driven one. The two rollers are connected by cellophane tape, which is made by transparent adhesive tape. All the pads are stuck on the tape. In the forward direction of the belt, the colloidal gold pad is put in the front and followed by an absorption pad with a distance of 11 mm. One colloidal gold pad and one absorption pad is used as a whole during the concentration process. The distance between the gold pad and one absorption pad is 20 mm without mutual interference. The strip without the colloidal gold pad and absorption pad are stuck to a baffle that can be moved powered by an electric machine. The control section consists of two electric machines: one is used to move the strip back and forth and the other one is in charge of the rolling of B. Two buttons are control switches for the electric machines.

Results and Discussion

The Structure and Working Principle of the Concentration Integrated Microfluidic LFA

In common LFAs, after adding the solution to the sample pad, the sample migrates with buffer through the strip by capillary forces and dissolves the report reagent in the conjugation pad. The conjugates flow forward in the porous membrane until they are captured by Abs immobilized on the test line (TL), giving a detectable signal. Redundant conjugates in the remaining solution flow through the membrane are attached to the control line (CL), showing the successful running of the test. Since the result of an LFA is related to the optical signal generated at the test line, the more amount of conjugates captured on the test line, the better detection of trace analyte will be. Although there is a comparatively excessive amount of Abs immobilized on the detection line, however, the bottleneck problem lies in the limited amount of conjugates that can be adsorbed and transferred by the sample pad and conjugated pad. After all, one piece of sample pad and conjugated pad with limited length cannot load and transfer much sample.

In this paper, a novel strategy by repeatedly replenishing the colloidal gold pad to realize on-stripe competitive injection and then multiple concentration was adopted with the aid of mechanic roller. The enrichment mechanism is shown in Fig. 2. With the accurate control of the step length and the race of rotation, a consistent length of the pad was assembled each time, guaranteeing the linearity between the amount of enrichment and number of rotation. The sample is added onto the sample pad through the injection pump for precise volume control.

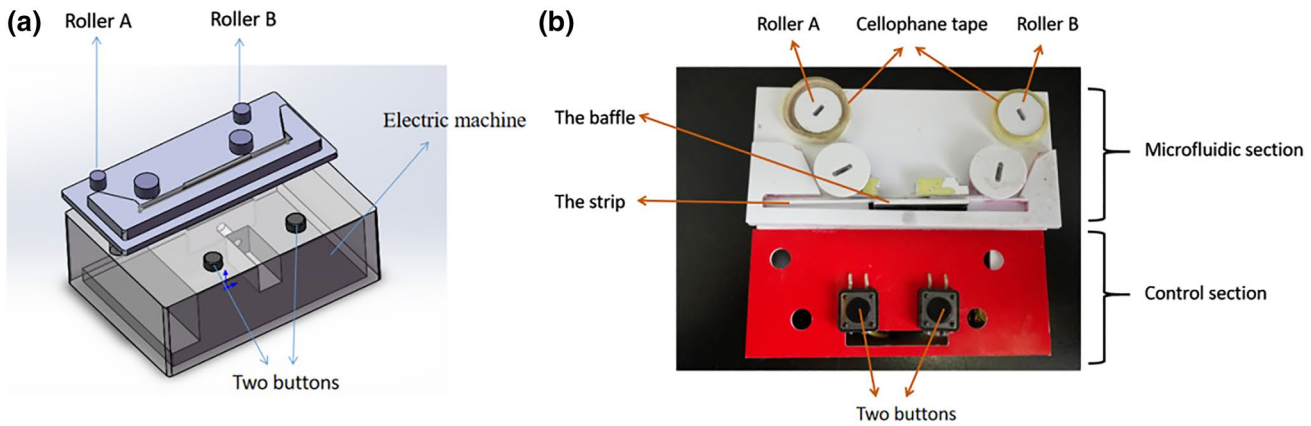

Fig. 1 **a** Design drawing of the device; **b** the structure of the microfluidic machine

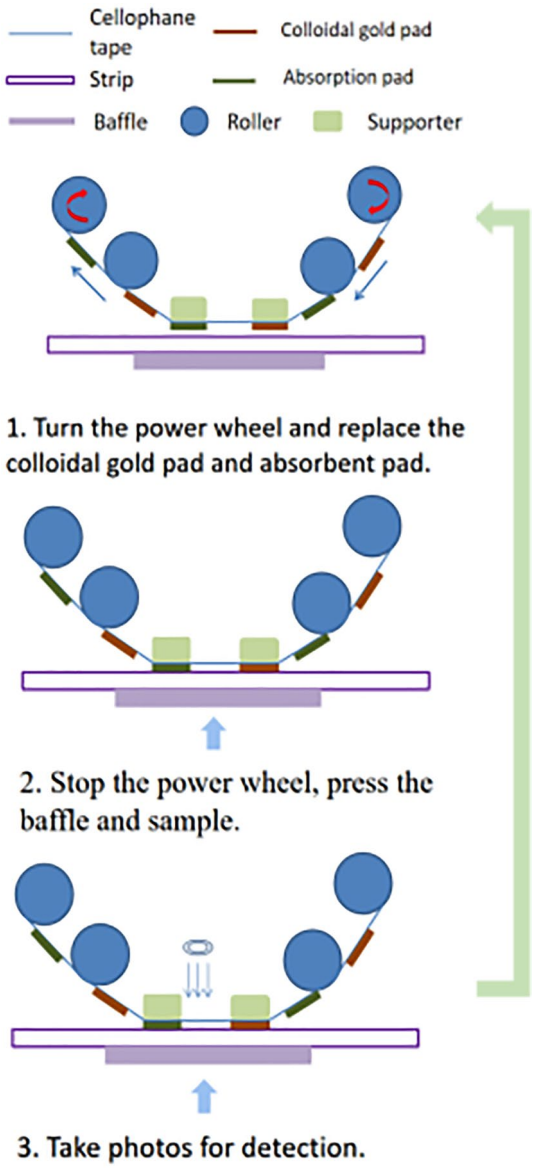

Fig. 2 The enrichment mechanism of our microfluidic lateral flow assay

The Optimization of Sample Amount

If the injection amount is too small, the amount of sample is not enough to in the detection area to give a detectable signal. If the sample amount is too large, an excessive amount of sample will enter the detection area without binding with colloidal gold and Abs on the test strip in the detection site, giving a lower signal than the real concentration of the sample. Therefore, a series volume of 10, 15, 20, and 25 μL of pure water were applied, respectively, to study the proper sample amount of test strip. It was shown that 10 μL of HCG could not make its way to the test strip, while a sample of 25 μL exceeded the water adsorption capacity of the test strip. Therefore, an injection in 15–20 μL was proper in this experiment, and 15 μL was chosen in the following experiment.

The Sample Analysis with the Proposed Device

The detection limit of commercial LAFs using the traditional method is 7.85 ng/mL. Using the proposed device in this paper, if the sample with a concentration of 7.85 ng/mL was five times diluted to 1.57 ng/mL, the sample could be detected. As shown in Fig. 4, in the first round of analysis of HCG sample in the concentration of 1.57 ng/mL, the textline (T-line) was almost invisible to the naked eye. After the five rounds of enrichment, red bands were seen with the naked eye. According to the detection limit of commercial LAFs, five-time enrichment of sample with the initial concentration of 1.57 ng/mL after five rounds of rotation had been realized.

The Study of the Linearity Between the Signal Intensity and Enrichment Times

The linearity between the signal intensity and enrichment times with the proposed device was further studied with the samples in the concentrations of 1.57 ng/mL and lower concentration of 1.26 ng/mL. The LAF images were analyzed with ImageJ software. The corresponding gray value of each band was given in Tables 1 and 2. As can be more easily

Table 1 Gray analysis of the detection image of HCG (1.57 ng/mL)

	1	2	3	4	5	6	7	8
Control line	29.688	39.509	40.969	48.962	50.921	78.489	76.009	72.279
Test line	4.181	7.587	8.292	8.259	10.219	13.712	15.538	18.448

Table 2 Gray analysis of the detection image of HCG (1.26 ng/mL)

	1	2	3	4	5	6	7	8	9
Control line	11.743	33.716	44.16	65.063	66.84	67.9	64.664	50.588	65.767
Test line	2.346	2.355	2.472	6.315	7.311	8.691	9.724	10.154	10.508

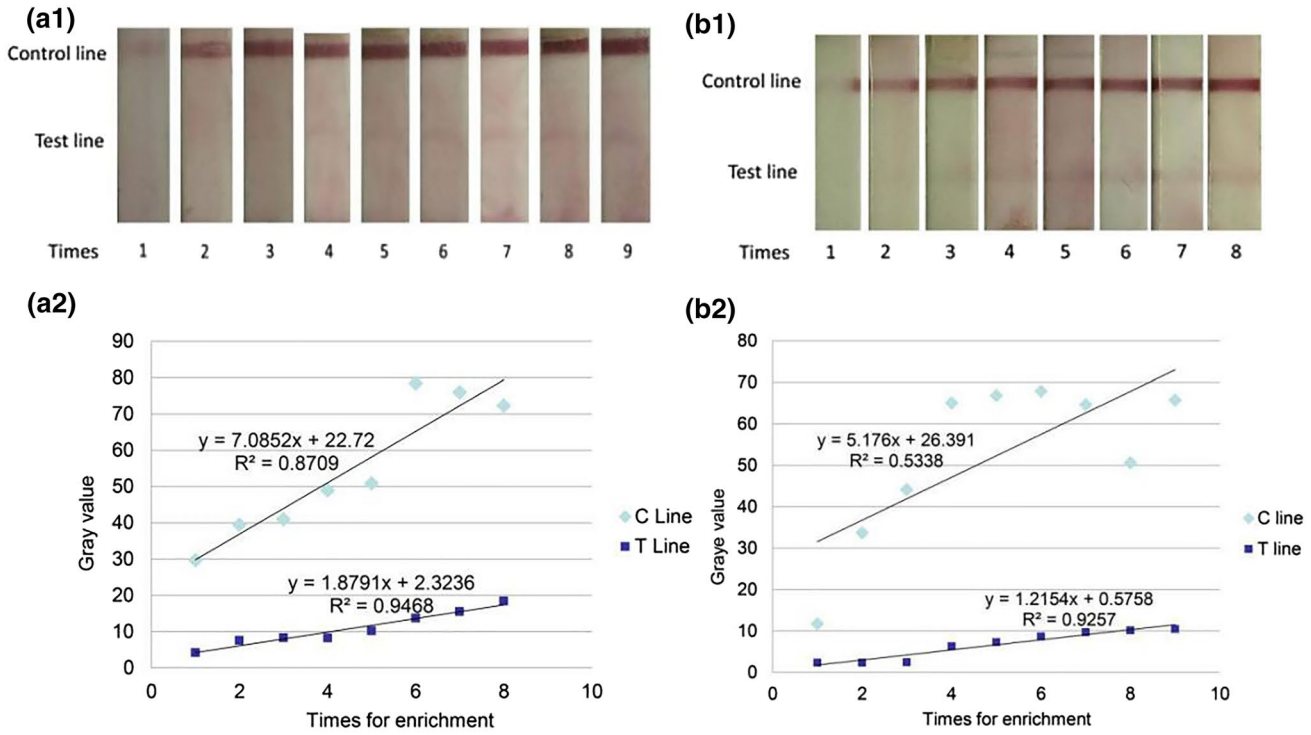

Fig. 3 **a1** LAF images of HCG in the concentration of 1.57 ng/mL; **a2** the linearity between the gray value of bands and the times for enrichment; **b1** LAF images of HCG in the concentration of 1.26 ng/mL; **b2** the linearity between the gray value of bands and the times for enrichment

observed in Fig. 3, there is a linear relationship between T-line and the control line (C-line), respectively, with the number of enrichment when the rounds of enrichment are smaller than five times. The R^2 value of 0.9468 and 0.9257 for the samples of 1.57 and 1.26 ng/mL, respectively, indicate that the enrichment effect was linearly and consistently correlated with the number of enrichment. The good linearity also indicated the super reproducibility of this mechanic device. When the enrichment times for the sample of 1.57 ng/mL were more than five times, there was no further enrichment due to the adsorption saturation of antibody on the C line. And it can also be observed, the range of linearity in the sample of 1.57 ng/mL was wider than the sample of 1.26 ng/mL. The detection in the lower concentration is more challenging. When the sample of 1.26 ng/mL was analyzed for several times, the approximate grey value of the C line obtained after five rounds of enrichment indicates the good reproducibility of the device. At the same time, the fixed amount of sample loss reflected also indicates that there is systemic error which makes it easier for future improvement.

The Study of the Relationship Between the Predicted Accumulation Quantity of HCG and the Gray Value of Bands

The results of multiple HCG enrichment integrated analysis were further compared between the different samples in the concentration of 1.26 and 1.57 ng/mL, respectively. According to the initial concentration of samples and times of concentration, a predicted accumulation quantity of HCG after five rounds of enrichment and the gray value of each band

Table 3 The comparison of HCG enrichment with the concentration of 1.26 and 1.57 ng/mL

Predicted accumulation quantity of HCG (ng)	0.019	0.024	0.038	0.047	0.057	0.071	0.075	0.094
Gray value (1.26 ng/mL)	2.346	–	2.355	–	2.472	–	6.315	7.311
Gray value (1.57 ng/mL)	–	4.181	–	7.587	–	8.292	–	8.259
Predicted accumulation quantity of HCG (ng)	0.113	0.118	0.132	0.142	0.151	0.165	0.170	0.189
Gray value (1.26 ng/mL)	8.691	–	9.724	–	10.154	–	10.508	–
Gray value (1.57 ng/mL)	–	10.219	–	13.712	–	15.538	–	18.448

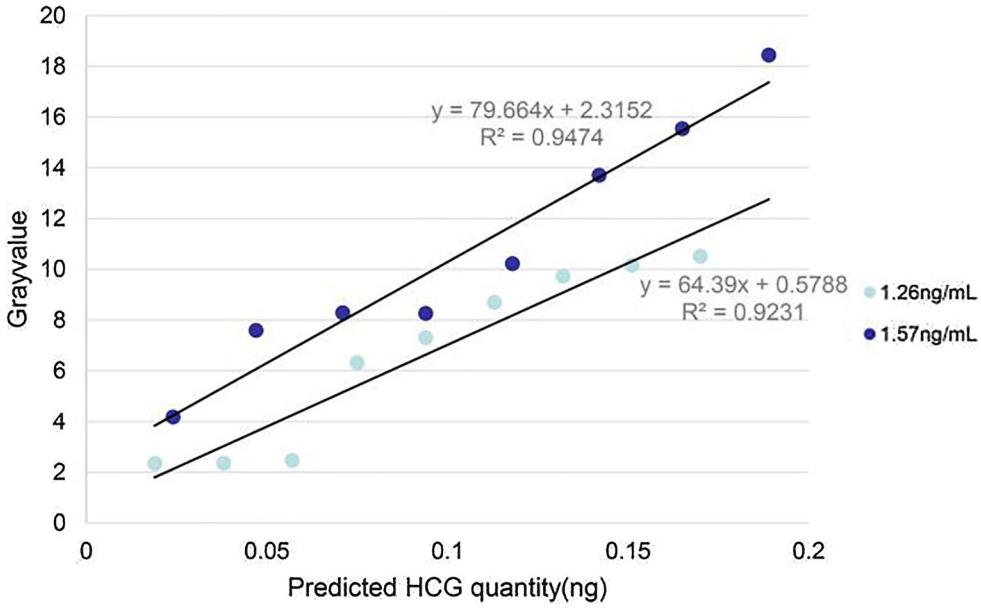

Fig. 4 The relationship between the predicted accumulation quantity of HCG and the gray value of bands

in the different concentration rounds are given together in Table 3. As can be observed in Fig. 4, the real grey value reflecting the actual amount of HCG is in the linearity with the predicted accumulation quantity of HCG, demonstrating again the good linear enrichment performance of the system and feasibility of semi-quantitative detection after further optimization.

Table 4 The summary of the LAFs detection limit for protein in literature

	Detection target	Detection limit	LAFs detection method
1	Tetanus antibody [33]	0.00011 IU/mL	Ultra-bright fluorescent nanospheres
2	Prostate-specific antigen (PSA) and human chorionic gonadotropin (hCG) [34]	0.1 ng mL(−1) of PSA and 1 ng mL(−1) of hCG	Persistent luminescent nanophosphors
3	Human chorionic gonadotropin [35]	2.8 mIU/mL	Plasmonic thermal sensing
4	Cardiac troponin I [36]	0.84 pg mL^{-1}	Enzyme-catalyzed chemiluminescence method, gold nanoparticles for enhanced enzyme conjugation and a mass-producible and time-programmable amplification part based on a water-swellable polymer for automating the sequential reactions in the immunoassay and signal amplification
5	Alpha-fetoprotein (AFP) [37]	9.2 pg mL(−1)	Surface-enhanced resonance Raman scattering (SERRS)-based lateral flow immunoassay (LFIA)
6	Human epidermal growth factor receptor 2 (HER2) [38]	20 nM	Aptamers and gold nanoparticles colorimetric lateral flow assay
7	Free and complexed prostate-specific antigen [39]	0.009 ng mL(−1) and 0.087 ng mL(−1), respectively.	Magnetic-quantum dot nanobeads as versatile fluorescent probes
8	Troponin [40]	0.019 ng mL(−1)	Fluorescent lateral flow immunoassay
9	C-reactive protein [41]	0.01 mu g mL(−1)	Imprinted polycarbonate sheets
10	Interleukin-6 [42]	1 pg/mL in PBS	SERS-based lateral flow assay
11	Glycoprotein [43]	7.02 ng mL(−1)	Gold-nanoparticle-decorated silica nanorod (Au@SiO2) nanocomposites based lateral flow immunoassay
12	Complement factor B [44]	5 ng mL(−1)	Magnetized Carbon Nanotube-Based Lateral Flow Immunoassay for Visual Detection

The Investigation of Detection Limit and Performance Comparison with Literature

Based on the above study, a series of samples in the concentration of 1.26, 0.94, and 0.63 ng/mL, respectively, lower than 1.57 ng/mL were studied. It was found that the sample in the concentration of 1.26 ng/mL could be detected. While there was not an obvious band in the analysis of the sample in the concentration of 0.94 ng/mL. And then, the detection limit of this proposed method for HCG was 1.26 ng/mL. The performance of this method is compared with LAFs for protein detection in the latest literature. As shown in Table 4, without the requirement of an extra instrument such as surface-enhanced resonance Raman scattering [5, 10], the detection limit obtained through the integration of ordinary LAFs with the simple microfluidic device in this paper is comparable with these method using special nanoparticles [6, 7, 11, 12].

Conclusions

The main focus of this technology nowadays is how to substantially improve LFA sensitivity without sacrificing its advantages. The existing improvements in LFA could be categorized into reaction, transport and signals [1]. In this paper, different from the existing way of improvement, with the advantage of chip integration, the sample pad was repetitively replaced to realize multi-enrichment of analyte onto the detection limit. This device was applied for enrichment detection of HCG. The minimum concentration of the sample initially determined by this device is 1.26 ng/mL, which is more than six times lower than the detection limit of the classic strip method (7.86 ng/mL) and also comparable with literatures using special nanoparticles. Together with good sensitivity, the linear relationship between the signal intensity vs the times of concentration and the predicted accumulation quantity of HCG vs the gray value of bands, lay a foundation for quantitative and semi-quantitative detection of low-abundant targets in real sample samples. This cost-effective, reusable, naked eye or smartphone readable, and robust device holds great potential as a candidate for medical diagnosis, home testing, food and environment monition.

Funding This study was supported by Special-Funded Program on National Key Scientific Instruments and Equipment Development of China Grant Nos (2012YQ04014005).

References

1. Bishop Joshua D, Hsieh Helen V, Gasperino David J (2019) Sensitivity enhancement in lateral flow assays: a systems perspective. Lab Chip 15:2486–2499
2. Urusov AE, Zherdev AV, Dzantiev BB (2019) Towards lateral flow quantitative assays: detection approaches. Biosensors 9(3):89
3. Jiang Nan, Ahmed Rajib, Damayantharan Mylon (2019) Lateral and vertical flow assays for point-of-care diagnostics. Adv Healthcare Mater 14:1900244
4. Preechakasedkit P, Siangproh W, Khongchareonporn N (2018) Development of an automated wax-printed paper-based lateral flow device for alpha-fetoprotein enzyme-linked immunosorbent assay. Biosens Bioelectron 102:27–32
5. Reid R, Chaterjee B, Das S (2020) Application of aptamers as molecular recognition elements in lateral flow assays for analytical applications. Analytical Biochem 113574
6. Tang R, Yang H, Gong Y (2017) A fully disposable and integrated paper-based device for nucleic acid extraction, amplification and detection. Lab Chip 7:1270–1279
7. Kwang WO, Lee K, Ahn B, Furlani EP (2012) Design of pressure-driven microfluidic networks using electric circuit analogy. Lab Chip 12(3):515–545
8. Safavieh R, Capillarics Juncker D (2013) Pre-programmed, self-powered microfluidic circuits built from capillary elements. Lab Chip 13(21):4180–4189
9. Kwang WO, Ahn CH (2006) A review of microvalves. J Micromech Microeng 16(5):R13–R39
10. Arango Y, Temiz Y, Gökçe O, Delamarche E (2018) Electrogates for stop-and-go control of liquid flow in microfluidics. Appl Phys Lett 112:153701
11. Corstjens PLAM, Nyakundi RK, De Dood CJ, Kariuki TM, Ochola EA, Karanja DMS, Mwinziand PNM, Van Dam GJ (2015) Improved sensitivity of the urine CAA lateral-flow assay for diagnosing active Schistosoma infections by using larger sample volumes. Parasites Vect 8:241
12. Zhengzong W, He D, Cui B (2019) Ultrasensitive detection of microcystin-LR with gold immunochromatographic assay assisted by a molecular imprinting technique. Food Chem 283:517–521
13. Mahmoudi T, de la Guardia M, Shirdel B (2019) Recent advancements in structural improvements of lateral flow assays towards point-of-care testing. Trac-trends Anal Chem 116:13–30
14. Strauch EM, Bernard SM, La D, Bohn AJ, Lee PS, Anderson CE, Nieusma T, Lee KK, Ward AB, Yager P, Fuller DH, Wilson IA, Baker D (2017) Computational design of trimeric influenza-neutralizing proteins targeting the hemagglutinin receptor binding site. Nat Biotechnol 35:667–671
15. Ilacas Grenalynn C, Basa Alexis, Nelms Katherine J (2019) Paper-based microfluidic devices for glucose assays employing a metal-organic framework (MOF). Anal Chim Acta 1055:74–80
16. Tang RH, Liu LN, Zhang SF, He XC, Li F (2019) A review on advances in methods for modification of paper supports for use in point-of-care testing. Microchim Acta 186(8)
17. Parolo C, Medina-Sánchez M, De La Escosura-Muñizand A, Merkoçin A (2013) Simple paper architecture modifications lead to enhanced sensitivity in nanoparticle based lateral flow immunoassays. Lab Chip 13:386–390
18. Tang R, Yang H, Gong Y, Liu Z, Li XJ, Wen T, Qu ZG, Zhang S, Mei Q, Xu F (2017) A fully disposable and integrated paper-based device for nucleic acid extraction, amplification and detection. Lab Chip 17(7):1270–1279
19. Rivas L, Medina-Sánchez M, De La Escosura-Muñiz A, Merkoçi A (2014) Improving sensitivity of gold nanoparticle-based lateral

flow assays by using wax-printed pillars as delay barriers of microfluidics. Lab Chip 14:4406–4414
20. Songjaroen T, Dungchai W, Chailapakul O, Henry CS, Laiwattanapaisal W (2012) Blood separation on microfluidic paper-based analytical devices. Lab Chip 12(18):3392–3398
21. Jui-Chuang W, Chen C-H, Ja-Wei F, Yang H-C (2014) Electrophoresis-enhanced detection of deoxyribonucleic acids on a membrane-based lateral flow strip using avian influenza H5 genetic sequence as the model. Sensors 3:4399–4415
22. Lung-Ming Fu, Hou Hui-Hsiung, Chiu Ping-Hsien, Yang Ruey-en (2018) Sample preconcentration from dilute solutions on micro/nanofluidic platforms: a review. Electrophoresis 39(2):289–310
23. Tang R, Yang H, Choi JR, Gong Y, Hu J, Feng S, Pingguan-Murphy B, Mei Q, Xu F (2016) Improved sensitivity of lateral flow assay using paper-based sample concentration technique. Talanta 152:269–276
24. Ghosh S, Ahn CH (2019) Lyophilization of chemiluminescent substrate reagents for high-sensitive microchannel-based lateral flow assay (MLFA) in point-of-care (POC) diagnostic system. Analyst 6:2109–2119
25. Yunhui Y, Mehmet O, Guodong L (2017) Gold nanocage-based lateral flow immunoassay for immunoglobulin G. Microchim Acta 184(7):2023–2029
26. Xu H, Chen J, Birrenkott J, Zhao JX, Takalkar S, Baryeh K, Liu G (2014) Gold-nanoparticle-decorated silica nanorods for sensitive visual detection of proteins. Anal Chem 86(15):7351–7359
27. Quesada-González D, Merkoçi A (2015) Nanoparticle-based lateral flow biosensors. Biosens Bioelectron 73:47–63
28. Grant D, Smith CA, Karvonen K, Richards-Kortum R (2016) Highly sensitive two-dimensional paper network incorporating biotin-streptavidin for the detection of malaria. Anal Chem 88:2553–2557
29. Gao Z, Ye H, Tang D (2017) Platinum decorated gold nanoparticles with dual functionalities for ultrasensitive colorimetric in vitro diagnostics. Nano Lett 9:5572–5579
30. Zhao Y, Huang Y, Zhao X, McClelland JF, Lu M (2016) Nanoparticle-based photoacoustic analysis for highly sensitive lateral flow assays. Nanoscale 8:19204–19210
31. Hwang J, Lee S, Choo J (2016) Application of a SERS-based lateral flow immunoassay strip for the rapid and sensitive detection of staphylococcal enterotoxin B. Nanoscale 8:11418–11425
32. Shi Q, Huang J, Sun Y, Deng R, Teng M, Li Q, Yang Y, Hu X, Zhang Z, Zhang G (2018) A SERS-based multiple immunonanoprobe for ultrasensitive detection of neomycin and quinolone antibiotics via a lateral flow assay. Microchim Acta 185:84
33. Chen J, Meng H-M, An Y, Liu J, Yang R, Lingbo Q, Li Z (2020) A fluorescent nanosphere-based immunochromatography test strip for ultrasensitive and point-of-care detection of tetanus antibody in human serum. Anal Bioanal Chem 412(5):1151–1158
34. Danthanarayana AN, Finley E, Binh V (2020) A multicolor multiplex lateral flow assay for high-sensitivity analyte detection using persistent luminescent nanophosphors. Anal Methods 12(3):272–280
35. Zhuo Q, Wang K, Alfranca G (2020) A plasmonic thermal sensing based portable device for lateral flow assay detection and quantification. Nanoscale Res Lett 15(1):10
36. Han G-R, Ki H, Kim M-G (2020) Automated, universal, and mass-producible paper-based lateral flow biosensing platform for high-performance point-of-care testing. ACS Appl Mater Interfaces 12(1):1885–1894
37. Luchun L, Jiangliu Y, Liu X (2020) Rapid, quantitative and ultrasensitive detection of cancer biomarker by a SERRS-based lateral flow immunoassay using bovine serum albumin coated Au nanorods. RSC Adv 10(1):271–281
38. Ranganathan V, Srinivasan S, Singh A (2020) An aptamer-based colorimetric lateral flow assay for the detection of human epidermal growth factor receptor 2 (HER2). Anal Biochem 588:113471
39. Rong Z, Bai Z, Jianing L (2019) Dual-color magnetic-quantum dot nanobeads as versatile fluorescent probes in test strip for simultaneous point-of-care detection of free and complexed prostate-specific antigen. Biosens Bioelectron 145
40. Natarajan S, Fengmei S, Jayaraj J (2019) A paper microfluidics-based fluorescent lateral flow immunoassay for point-of-care diagnostics of non-communicable diseases. Analyst 144(21):6291–6303
41. Aoyama S, Monden K, Akiyama Y (2019) Enhanced immunoadsorption on imprinted polymeric microstructures with nanoengineered surface topography for lateral flow immunoassay systems. Anal Chem 91(21):13377–13382
42. Wang Y, Sun J, Hou Y (2019) A SERS-based lateral flow assay biosensor for quantitative and ultrasensitive detection of interleukin-6 in unprocessed whole blood. Biosens Bioelectron 141
43. Hui X, Zheng L, Xie Y (2019) Identification and determination of glycoprotein of edible brid's nest by nanocomposites based lateral flow immunoassay. Food Control 102:214–220
44. Huang Y, Wu T, Wang F (2019) Magnetized carbon nanotube-based lateral flow immunoassay for visual detection of complement factor B. Molecules 24(15)